



Enhancement of efficiency of InGaN-based light emitting diodes through strain and piezoelectric field management

J. Pal, M. A. Migliorato, C.-K. Li, Y.-R. Wu, B. G. Crutchley, I. P. Marko, and S. J. Sweeney

Citation: [Journal of Applied Physics](#) **114**, 073104 (2013); doi: 10.1063/1.4818794

View online: <http://dx.doi.org/10.1063/1.4818794>

View Table of Contents: <http://scitation.aip.org/content/aip/journal/jap/114/7?ver=pdfcov>

Published by the [AIP Publishing](#)



Re-register for Table of Content Alerts

Create a profile.



Sign up today!



Enhancement of efficiency of InGaN-based light emitting diodes through strain and piezoelectric field management

J. Pal,¹ M. A. Migliorato,¹ C.-K. Li,² Y.-R. Wu,² B. G. Crutchley,³ I. P. Marko,³
 and S. J. Sweeney³

¹*School of Electrical and Electronic Engineering, University of Manchester, Manchester, United Kingdom*

²*Graduate Institute of Photonics and Optoelectronics and Department of Electrical Engineering, National Taiwan University, Taipei 10617, Taiwan*

³*Advanced Technology Institute and Department of Physics, University of Surrey, Guildford, Surrey GU2 7XH, United Kingdom*

(Received 12 June 2013; accepted 1 August 2013; published online 21 August 2013)

We report calculations of the strain dependence of the piezoelectric field within InGaN multi-quantum wells light emitting diodes. Such fields are well known to be a strong limiting factor of the device performance. By taking into account the nonlinear piezoelectric coefficients, which in particular cases predict opposite trends compared to the commonly used linear coefficients, a significant improvement of the spontaneous emission rate can be achieved as a result of a reduction of the internal field. We propose that such reduction of the field can be obtained by including a metamorphic InGaN layer below the multiple quantum well active region. © 2013 AIP Publishing LLC.

[<http://dx.doi.org/10.1063/1.4818794>]

I. INTRODUCTION

Strong advances in the growth and device fabrication of nitride semiconductors have led to major improvements of InGaN light emitters in recent years. Solid State lighting, displays, laptop and television back lighting, blue-ray players, pico-projection systems, traffic signal, and automotive applications are a few of the applications which have caused considerable interest in the development of InGaN-based light emitting diodes (LEDs).^{1–10} Continuing improvements in the performance of the InGaN emitters, particularly for green LEDs, are required in order to achieve the full market potential of InGaN-based emitters. One of the major factors limiting the light output power is the presence of in-built polarization fields that originate from the wurtzite crystal structure of III-N semiconductors.^{11–14} Such fields can be high enough to localize carriers at the interfaces and create, through Coulomb repulsion, energy barriers that hinder carrier transportation. With the aim of circumventing such issues, much work has recently been concentrated on understanding how to manage piezoelectric polarization in InGaN/GaN superlattices¹⁵ or producing devices on substrates with non-polar and semi-polar crystal orientations.^{16–19} However, the output powers at high injection current of these devices currently do not outperform the best devices grown on (0001) planes (c-planes).^{2,14,20,21}

II. METHODOLOGY

The device performance would be strongly enhanced if such fields were sizeably reduced in InGaN c-plane grown structures which are currently grown on either sapphire or silicon substrates. We have recently shown²² that experimentally there appears to be a linear correlation between the change in internal field and the reduction of the efficiency in c-plane GaN-based LED devices. This was revealed using optical efficiency measurements as a function of applied hydrostatic pressure of commercially available blue and

green polar multi-quantum well (MQW) LEDs with indium content of 14% and 26%, respectively, well widths of 3 nm in both LED types, and barrier widths of 13 nm in blue and 16 nm in green LEDs. Applying pressure (hydrostatic compressive strain) from 0 to 1 GPa led to a reduction of ~4% in the light output power for both LEDs at an operating current of 260 mA. In order to correlate this effect with the value of the polarization field, we estimated that the piezoelectric fields in the quantum well region have been calculated using both the linear piezoelectricity (LP) model of Bernardini and Fiorentini²³ and the more complete recently reported nonlinear piezoelectricity^{24–28} model (NLP) of Pal *et al.*²⁹

We reported²² that the LP model predicts a reduction of the field of around 2%, which should result in increased optical efficiency, which is the opposite effect to the experimental observations. In contrast, the NLP model predicts an increase of 4% in the strength of the piezoelectric field which is consistent with our experimental observations of a decrease in the optical efficiency by the same amount with increasing hydrostatic pressure. Whilst we observe an inverse proportionality and linear scaling between the efficiency and the value of the piezoelectric field in the active region as calculated using the NLP model, the radiative recombination rate is expected to show a stronger (quadratic rather than linear) increase with reducing internal polarization field strength due to the enhancement of the optical matrix element in Fermi's golden rule. This discrepancy can be attributed to the fact that the experimental output power is increased by the radiative recombination rate but decreased due to non-radiative processes,³⁰ resulting, in this case, in an approximately linear rather than quadratic dependence on the applied pressure.

We now investigate the dependence of the internal field on applied tetragonal pressure, i.e., a combination of tensile (in the growth plane) and compressive (along the c-axis) strain, instead of hydrostatic pressure, which is equal in all directions, used in our experiments.

The calculations are performed in a similar framework as previously used.²⁹ This time, in addition, we also included the effects of non-linear elasticity (NLE)³¹ which have been recently reported to be very important in order to correctly reproduce optical experimental data for nitride based LED structures.³²

We studied a typical active region of a LED structure containing a series of $\text{In}_x\text{Ga}_{1-x}\text{N}/\text{GaN}$ multi quantum wells grown on a GaN layer, assuming that no residual strain from the substrate is present. For blue and green emission, we used indium compositions of $x = 0.14$ and $x = 0.26$, respectively, and a typical structure with a 3 nm/3 nm well to barrier ratio. The built-in field in the quantum well region can be estimated from the super-lattice equation

$$F_{PZ} = \frac{(P_b - P_w)}{\varepsilon_w + \varepsilon_b(L_w/L_b)}, \quad (1)$$

where $L_{b,w}$ are the widths of the barrier and well, $P_{b,w}$ are the polarizations of the barrier and well, and $\varepsilon_{b,w}$ is the dielectric constants of the barrier and well.

The total polarization in the barrier and well regions is given by the quadratic expression

$$P_{Tot} = P_{sp} + e_{33}\varepsilon_{\perp} + 2e_{31}\varepsilon_{//} + e_{311}\varepsilon_{//}^2 + e_{333}\varepsilon_{\perp}^2 + e_{313}\varepsilon_{//}\varepsilon_{\perp}, \quad (2)$$

where P_{sp} is the spontaneous polarization, $\varepsilon_{//}$ and ε_{\perp} refer to strain in c-plane and in the orthogonal direction, respectively. The coefficients e_{ij} and e_{ijk} are the NLP coefficients, taken from Pal *et al.*²⁹

The relation between parallel and perpendicular strain components is evaluated using the following equations:³⁰

$$C_{\alpha\beta}(P) = \sum_{n=1}^4 C_{\alpha\beta,i} P^n, \quad (3)$$

$$\varepsilon_{\perp} = -\frac{2C_{13}(P)}{C_{33}(P)}\varepsilon_{//}, \quad (4)$$

where P is the internal pressure, $C_{\alpha\beta,i}$ are the NLE parameters, and $C_{\alpha\beta}(P)$ are the final pressure dependent elastic parameters, taken from Lepkowski.³¹

III. RESULTS

In Figure 1, we show the dependence of the total polarization (spontaneous plus strain induced polarization) in the well and barrier region as a function of tensile strain (evaluated from NLE) in the plane orthogonal to the c-axis for the blue (a) and the green (b) LED structures. Note that vanishing tensile stress in this plot equates to the situation encountered in devices when the entire structure is lattice matched in the c-plane to the GaN lattice parameter. Essentially, the tensile strain on the abscissa of the graph needs to be interpreted as an additional tensile strain but not as the overall strain. Therefore, the polarization results from the parallel strain due to the lattice mismatch between the bulk values of the InGaN and GaN lattice parameters and an additional (hypothetical) tensile strain. However, we have also taken into

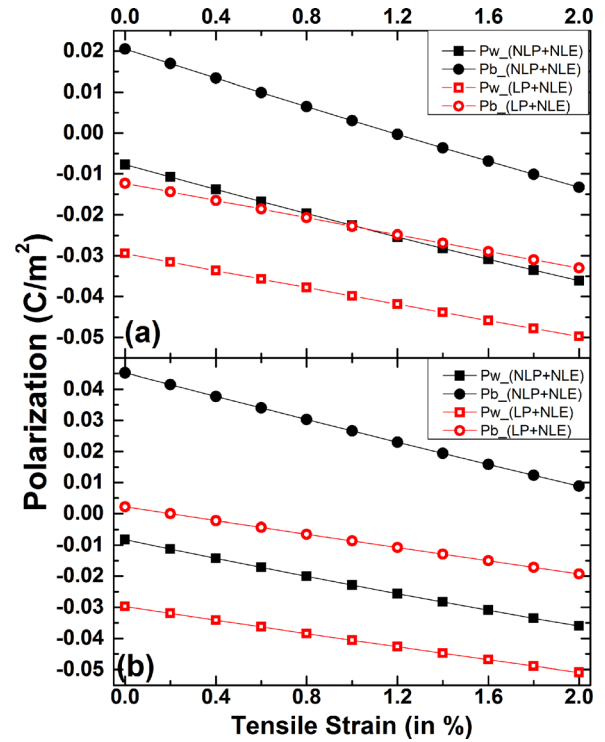


FIG. 1. Dependence of the total polarization (spontaneous plus strain induced polarization) in the well and barrier region as a function of tensile strain (evaluated from NLE) in the c-plane for both the blue (a) and the green (b) LED structures.

account any additional compressive strain in the c-axis originating from the additional tensile strain in the c-plane. Though both well and barrier polarizations, for both blue and green LED structures, show a similar slope as a function of additional tensile strain, the magnitude of the polarizations, when calculated using LP and NLP parameters, are substantially different. This is primarily a result of the much smaller spontaneous polarization terms of NLP compared to LP. In both cases of blue and green LEDs, the polarization calculated with NLP is always stronger (more positive) than that calculated with LP.

Significant differences between the two models arise when the polarizations shown in Fig. 1 are used with the superlattice equation (Eq. (1)) in order to calculate the fields in the barrier and well regions. In Fig. 2, we show the dependence of the piezoelectric field in the MQW region as a function of the tensile strain in the c-plane as used in Fig. 1 for both the blue and the green LED structures calculated using Eq. (1). For comparison, we show the results obtained using the LP model, the NLP model, and the NLP model with the addition of NLE. Unlike LP, the NLP model combined with NLE leads to a pronounced reduction of the piezoelectric field as a function of increasing tensile strain in the well region. For example, a 1% additional tensile strain would result in a change of the piezoelectric field from 1.54 MV cm^{-1} to 1.40 MV cm^{-1} in the blue LED and from 2.825 MV cm^{-1} to 2.615 MV cm^{-1} in the green LED. Such reduction is also larger compared with the case of using the NLP model with LE.

On the top axis of Fig. 2, we show the In composition of a relaxed $\text{In}_x\text{Ga}_{1-x}\text{N}$ intermediate layer (see Fig. 3) between

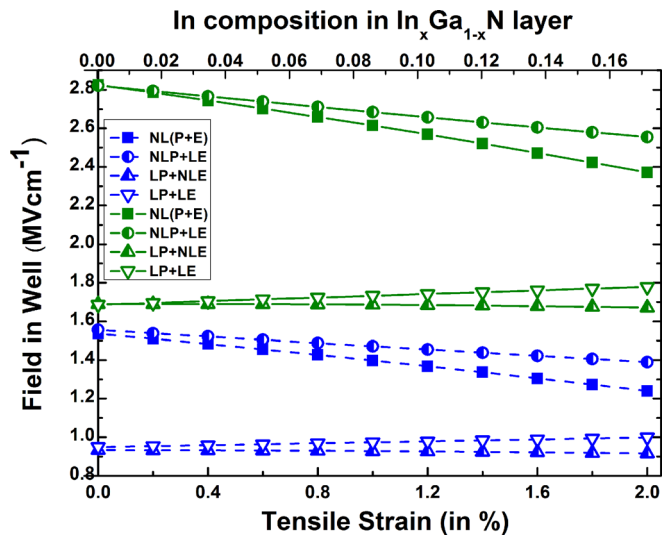


FIG. 2. Dependence of the piezoelectric field in the well region as a function of tensile strain in the *c* plane, for both the blue and the green LED structures. We compare the calculations using the LP model, the NLP model, and the NLP model with the addition of NLE.

the substrate and LED structure which would generate the corresponding additional tensile strain as shown on the bottom axis. Thus, if the MQW region was grown on a relaxed In_{0.09}Ga_{0.91}N layer, then an additional tensile strain of around 1% in the growth plane would be present throughout the active region of the device.

Our data suggest that one effective way to reduce the detrimental effects of the presence of internal piezoelectric fields inside the active region of *c*-plane of InGaN LED

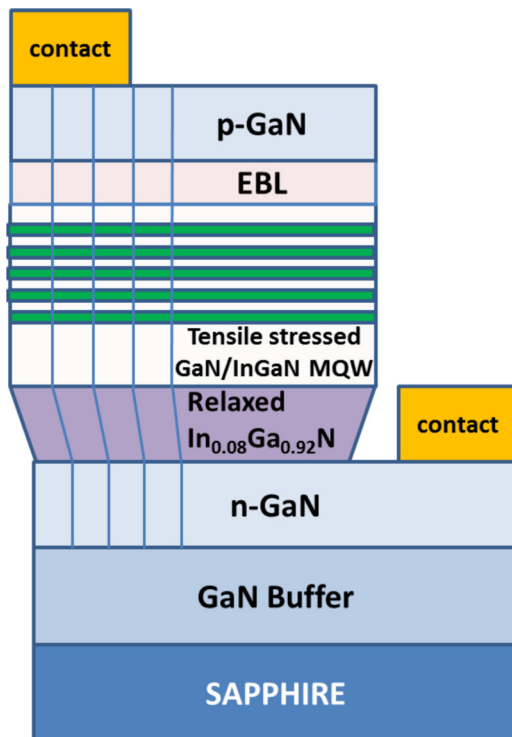


FIG. 3. Proposed *c* plane InGaN LED device structure using a metamorphic layer before the MQW region which is grown on the top of *n*-type GaN layer. The InGaN quantum well has either 14% or 26% for the blue or green emission, respectively.

devices is to use an InGaN metamorphic layer (Fig. 3). The compositions proposed of up to 9% In are in the achievable range for crystal growth. Metamorphic layers have been demonstrated³³ to start strained and lattice matched to the substrate while subsequently relaxing towards their bulk lattice parameter, providing a virtual substrate on which the new layers then can be grown. Partial relaxation after about 10–20 nm seems to favour the growth of subsequent layers lattice matched with the new virtual substrate. In this way, with the metamorphic layer inserted before the MQW region, the subsequently deposited material would feel a strain reduction in the InGaN layers and a strain increase in the GaN barriers.

Inevitably, such a layer could provide an additional source of dislocations (though it could also stop threading dislocations propagating from the substrate), it would also substantially reduce the piezoelectric field in the active region. Additionally, the large conduction band discontinuity between InGaN and GaN can affect mobility of the *n*-type carriers,³⁴ but since the problem in bipolar devices such as LEDs is with hole transport, it should not significantly affect device performance. Since a 1% additional tensile strain reduces the internal field by ~9% and ~8% for the blue and green LEDs, respectively, and since we have showed how a field reduction can be linked to a comparable increase in optical efficiency,²² we believe that a metamorphic intermediate InGaN layer could produce significant benefits for improved device performance.

Having all the recent advances and increased level of control achieved in crystal synthesis and metalorganic chemical vapour deposition growth of nitride compounds, the inclusion of a relaxed layer of InGaN with a modest In concentration is simply a matter of experimentally finding the correct growth conditions. Furthermore, it should also make the deposition of the MQW region easier as it would reduce the lattice mismatch between the well and barrier regions. Such an increased tensile strain as in our proposed structure in Fig. 3 is likely to vanish in the subsequent layers deposited after the MQW region, due to the typically large thickness. Therefore, one can expect that the electronic blocking layer (EBL) and *p*-doped GaN region could be grown without additional need to significantly alter growth conditions compared to the case where the metamorphic layer was not included.

It is also worth mentioning that though direct comparison is difficult, these prediction had to some extent already been made by Shieh *et al.*,¹⁵ who by modelling the band offsets and interface polarization of InN/GaN superlattices as a function of strain had concluded that the strain conditions were an unrecognized degree to which device properties could be potentially controlled.

To further test our proposal, we calculated the spontaneous emission spectra for the green and blue LEDs with and without the metamorphic layer. We utilized a self-consistent Poisson and $6 \times 6 \mathbf{k} \cdot \mathbf{p}$ Schrödinger solver to solve the quantum well band structures iteratively until convergence. The $6 \times 6 \mathbf{k} \cdot \mathbf{p}$ method^{35–37} is used for calculating the valence band levels. The conduction band levels are calculated by the effective mass approximation. We use the polarization-dependent optical matrix elements

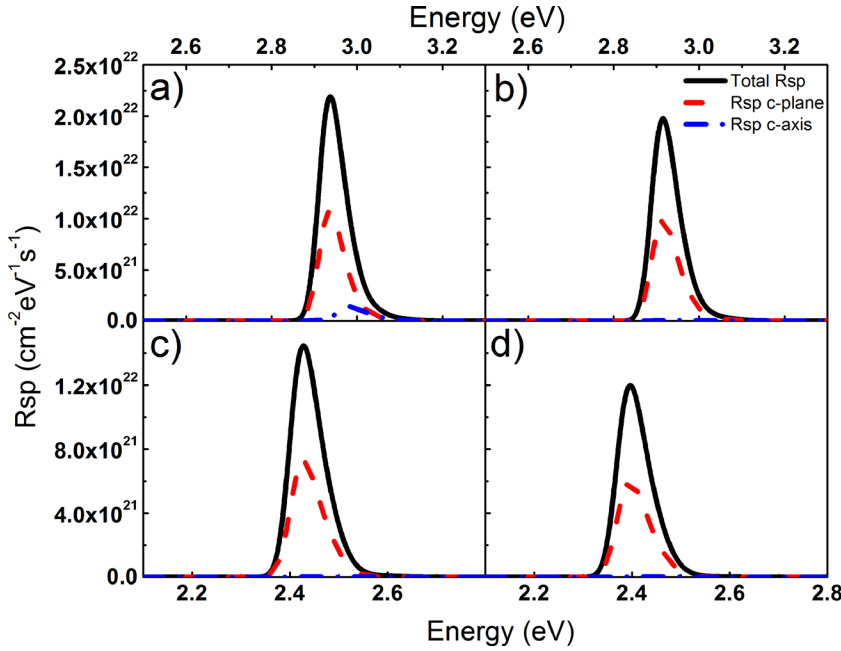


FIG. 4. Spontaneous emission spectra at injection carrier density equal to $2.5 \times 10^{12} \text{ cm}^{-2}$ for both the blue ($x = 14\%$) and green ($x = 26\%$) LED structures having $\text{In}_x\text{Ga}_{1-x}\text{N}/\text{GaN}$ quantum wells with metamorphic layer ((a) and (c)) and the conventional quantum well structure ((b) and (d)).

$$\begin{aligned}
 x - \text{polarized} &: |\langle S|p_x|X\rangle|^2 (|\langle \psi_l^e|\psi_{m1}^h\rangle\uparrow + \langle \psi_l^e|\psi_{m5}^h\rangle\uparrow|^2 + |\langle \psi_l^e|\psi_{m2}^h\rangle\downarrow + \langle \psi_l^e|\psi_{m6}^h\rangle\downarrow|^2)/4, \\
 y - \text{polarized} &: |\langle S|p_y|Y\rangle|^2 (|\langle \psi_l^e|\psi_{m1}^h\rangle\uparrow - \langle \psi_l^e|\psi_{m5}^h\rangle\uparrow|^2 + |\langle \psi_l^e|\psi_{m2}^h\rangle\downarrow - \langle \psi_l^e|\psi_{m6}^h\rangle\downarrow|^2)/4, \\
 z - \text{polarized} &: |\langle S|p_z|Z\rangle|^2 (|\langle \psi_l^e|\psi_{m3}^h\rangle\uparrow + \langle \psi_l^e|\psi_{m4}^h\rangle\downarrow|^2)/2,
 \end{aligned} \tag{5}$$

in the expression for the spontaneous emission rate,³⁸ which for electron-hole pair recombination in a quantum-confined active region is given by (in Gaussian units)

$$\begin{aligned}
 R_{sp} &= \int d(\hbar\omega) \frac{4\pi^2 e^2 \hbar}{n^2 m_0^2 \hbar \omega} \frac{1}{2\pi^2} \sum_{n,m} \int dk \sum_{\sigma,\hat{\epsilon}} |\hat{\epsilon} P_{nm}^\sigma(k)|^2 \\
 &\times \rho_{\hat{\epsilon}}(\hbar\omega) \delta(E_n^e(k) - E_m^h(k) - \hbar\omega) \\
 &\times [f^e(E_n^e(k))][1 - f^h(E_m^h(k))],
 \end{aligned} \tag{6}$$

where $\rho_{\hat{\epsilon}}$ is the (in general) polarization-dependent photon density of states.

In Fig. 4, we show the difference in emission strength, by comparison of the spontaneous emission spectra for both the blue ($x = 14\%$) and green ($x = 26\%$) LED structures having $\text{In}_x\text{Ga}_{1-x}\text{N}/\text{GaN}$ quantum wells with metamorphic layer

TABLE I. Wavefunction overlap, peak emission energy, peak spontaneous emission rate and integrated spontaneous emission for both the blue ($x = 14\%$) and green ($x = 26\%$) LED structures having $\text{In}_x\text{Ga}_{1-x}\text{N}/\text{GaN}$ quantum wells with and without metamorphic layer.

LED structure	Overlap $ \psi_e \psi_h $	Emission energy (eV)	Peak spontaneous emission rate $R_{sp}(\text{max}) 10^{22}$ ($\text{cm}^{-2} \text{eV}^{-1} \text{s}^{-1}$)	Integral of spontaneous emission rate (R_{sp}) 10^{21} ($\text{cm}^{-2} \text{s}^{-1}$)
Blue with ML	0.5070	2.94	2.190	1.801
Blue without ML	0.4525	2.92	1.975	1.619
Green with ML	0.3652	2.42	1.447	1.214
Green without ML	0.3329	2.40	1.197	1.003

(Figs. 4(a) and 4(c)) and the conventional quantum well (Figs. 4(b) and 4(d)).

At injection carrier density, n_{2D} , equal to $2.5 \times 10^{12} \text{ cm}^{-2}$, the conventional LED structures light emissions are significantly lower than the proposed ones with the metamorphic layer. The results are summarized in Table I.

The results clearly indicate that the addition of tensile strain to the active region is beneficial to the efficiency of LED devices. We also noticed that a similar proposition was experimentally reported by Zhang and Tansu,³⁹ who used InGaIn substrates with In composition of 15%. Such substrate would act precisely as the metamorphic layer proposed in this work. Zhang and Tansu³⁹ reported that the structure grown on InGaIn substrate exhibited spontaneous emission rates twice or thrice as large as the conventional structures. We can now theoretically confirm their result and the interpretation given by Zhang and Tansu,³⁹ who attributed the improved performance to an interplay between strain and internal polarization fields. However, we need to stress that only the nonlinear theory of piezoelectricity calculates correctly the reduction in the polarization field in the quantum well regions that is the origin of the increased spontaneous emission rate.

IV. CONCLUSION

In conclusion, we have analyzed the strain dependence of the piezoelectric field in the active region of two pseudo-morphically strained $\text{In}_x\text{Ga}_{1-x}\text{N}$ MQWs with different In content and designed for blue ($x = 0.14$) and green ($x = 0.26$) light emission. A significant reduction of the total internal piezoelectric field as a function of tensile strain is

found in both cases, when both non-linear piezoelectricity and non-linear elasticity models are taken into account in the calculations. Since tensile strain could be generated by growing the QW region on a semiconductor layer with a lattice parameter larger than that of GaN, a proposal to use a relaxed InGaN metamorphic layer has been presented. We have evaluated the optical matrix elements and the resulting spontaneous emission rate for the proposed structures and confirmed that, consistent with experimental data in the literature, an increase of the optical emission can be predicted. Since we have previously experimentally showed that the change in value of the internal piezoelectric fields is proportional to the change in optical efficiency, LED devices made using the proposed structures are expected to increase their light output power by up to 10%.

ACKNOWLEDGMENTS

The work is partially supported by National Science Council in Taiwan under grant No. NSC102-2221-E-002-194-MY3.

- ¹J. K. Kim and E. F. Schubert, *Opt. Express* **16**, 21835–21842 (2008).
- ²T. Mukai, M. Yamada, and S. Nakamura, *Jpn. J. Appl. Phys., Part 1* **38**, 3976 (1999).
- ³S. Nakamura, T. Mukai, and M. Senoh, *Appl. Phys. Lett.* **64**, 1687 (1994).
- ⁴U. Strauß, S. Brüninghoff, M. Schillgalies, C. Vierheilig, N. Gmeinwieser, V. Kümmler, G. Brüderl, S. Lutgen, A. Avramescu, D. Queren, D. Dini, C. Eichler, A. Lell, and U. T. Schwarz, *Proc. SPIE* **6894**, 689417 (2008).
- ⁵M. Funato, T. Kondou, K. Hayashi, S. Nishiura, M. Ueda, Y. Kawakami, Y. Narukawa, and T. Mukai, *Appl. Phys. Express* **1**, 011106 (2008).
- ⁶Z. C. Feng, *III-Nitride Devices and Nanoengineering* (Imperial College Press, London, 2008).
- ⁷E. F. Schubert, *Light-Emitting Diodes* (Cambridge University Press, 2003).
- ⁸M. H. Crawford, *IEEE J. Sel. Top. Quantum Electron.* **15**, 1028–1040 (2009).
- ⁹Y. F. Cheung and H. W. Choi, *IEEE Trans. Electron Devices* **60**, 333–338 (2013).
- ¹⁰T.-H. Wang and Y.-K. Kuo, *IEEE Photonics Technol. Lett.* **24**, 2084–2086 (2012).
- ¹¹S. Chichibu, T. Azuhata, T. Sota, and S. Nakamura, *Appl. Phys. Lett.* **69**, 4188 (1996).
- ¹²T. Takeuchi, S. Sota, M. Katsuragawa, M. Komori, H. Takeuchi, H. Amano, and I. Akasaki, *Jpn. J. Appl. Phys., Part 2* **36**, L382–L385 (1997).
- ¹³M.-H. Kim, M. F. Schubert, Q. Dai, J. K. Kim, E. F. Schubert, J. Piprek, and Y. Park, *Appl. Phys. Lett.* **91**, 183507 (2007).
- ¹⁴S. Huang, Z. Chen, Y. Xian, B. Fan, Z. Zheng, Z. Wu, H. Jiang, and G. Wang, *Appl. Phys. Lett.* **101**, 041116 (2012).
- ¹⁵C. C. Shieh, X. Y. Cui, B. Delley, and C. Stampfl, *J. Appl. Phys.* **109**, 083721 (2011).
- ¹⁶X. Li, X. Ni, H. Y. Liu, F. Zhang, S. Liu, J. Lee, V. Avrutin, Ü. Özgür, T. Paskova, G. Mulholland, K. R. Evans, and H. Morkoç, *Phys. Status Solidi C* **8**, 1560–1563 (2011).
- ¹⁷H. Masui, S. Nakamura, S. P. DenBaars, and U. K. Mishra, *IEEE Trans. Electron Devices* **57**, 88 (2010).
- ¹⁸Y. Kawaguchi, C.-Y. Huang, Y.-R. Wu, Q. Yan, C.-C. Pan, Y. Zhao, S. Tanaka, K. Fujito, D. Feezell, C. G. Van de Walle, S. P. DenBaars, and S. Nakamura, *Appl. Phys. Lett.* **100**, 231110 (2012).
- ¹⁹S. Takagi, Y. Enya, T. Kyono, M. Adachi, Y. Yoshizumi, T. Sumitomo, Y. Yamanaka, T. Kumano, S. Tokuyama, K. Sumiyoshi, N. Saga, M. Ueno, K. Katayama, T. Ikegami, T. Nakamura, K. Yanashima, H. Nakajima, K. Tasai, K. Naganuma, N. Futagawa, Y. Takiguchi, T. Hamaguchi, and M. Ikeda, *Appl. Phys. Express* **5**, 082102 (2012).
- ²⁰M. J. Lai, M. J. Jeng, and L. B. Chang, *Jpn. J. Appl. Phys., Part 1* **49**, 021004 (2010).
- ²¹T. Detchprohm, M. Zhu, W. Zhao, Y. Wang, Y. Li, Y. Xia, and C. Wetzel, *Phys. Status Solidi C* **6**, S840–S843 (2009).
- ²²B. G. Crutchley, I. P. Marko, S. J. Sweeney, J. Pal, and M. A. Migliorato, *Phys. Status Solidi B* **250**, 698–702 (2013).
- ²³F. Bernardini and V. Fiorentini, *Appl. Phys. Lett.* **80**, 4145 (2002).
- ²⁴G. Vaschenko, C. S. Menoni, D. Patel, C. N. Tomé, B. Clausen, N. F. Gardner, J. Sun, W. Götz, H. M. Ng, and A. Y. Cho, *Phys. Status Solidi B* **235**, 238 (2003).
- ²⁵D. Cai and G.-Y. Guo, *J. Phys. D: Appl. Phys.* **42**, 185107 (2009).
- ²⁶K. Shimada, T. Sota, K. Suzuki, and H. Okumura, *Jpn. J. Appl. Phys., Part 2* **37**, L1421 (1998).
- ²⁷G. Vaschenko, D. Patel, C. S. Menoni, N. F. Gardner, J. Sun, W. Götz, C. N. Tomé, and B. Clausen, *Phys. Rev. B* **64**, 241308 (2001).
- ²⁸O. Ambacher, J. Majewski, C. Miskys, A. Link, M. Hermann, M. Eickhoff, M. Stutzmann, F. Bernardini, V. Fiorentini, V. Tilak, B. Schaff, and L. F. Eastman, *J. Phys.: Condens. Matter* **14**, 3399 (2002).
- ²⁹J. Pal, G. Tse, V. Haxha, M. A. Migliorato, and S. Tomić, *Phys. Rev. B* **84**, 085211 (2011).
- ³⁰A. R. Adams, M. Silver, and J. Allam, *High Pressure in Semiconductor Physics II* (Academic, New York, 1998), Vol. 55, pp. 310–311.
- ³¹S. P. Lepkowski, *Phys. Rev. B* **75**, 195303 (2007).
- ³²T. Suski, S. P. Lepkowski, G. Staszczak, R. Czernecki, P. Perlin, and W. Bardyszewski, *J. Appl. Phys.* **112**, 053509 (2012).
- ³³N. Okamoto, K. Hoshino, N. Hara, M. Takikawa, and Y. Arakawa, *J. Cryst. Growth* **272**, 278 (2004).
- ³⁴C. X. Wang, K. Tsubaki, N. Kobayashi, T. Makimoto, and N. Maeda, *Appl. Phys. Lett.* **84**, 2313 (2004).
- ³⁵S. Ghosh, P. Waltereit, O. Brandt, H. T. Grahn, and K. H. Ploog, *Phys. Rev. B* **65**, 075202 (2002).
- ³⁶H.-H. Huang and Y.-R. Wu, *J. Appl. Phys.* **107**, 053112 (2010).
- ³⁷P.-Y. Dang and Y.-R. Wu, *J. Appl. Phys.* **108**, 083108 (2010).
- ³⁸I. Vurgaftman and J. Singh, *Appl. Phys. Lett.* **64**, 1472 (1994).
- ³⁹J. Zhang and N. Tansu, *J. Appl. Phys.* **110**, 113110 (2011).